Supplement of Biogeosciences, 15, 6461–6480, 2018
https://doi.org/10.5194/bg-15-6461-2018-supplement

Biogeosciences Open Access EGU

Supplement of

Evaluation of the seasonal formation of subsurface negative preformed nitrate anomalies in the subtropical North Pacific and North Atlantic

Robert T. Letscher and Tracy A. Villareal

Correspondence to: Robert T. Letscher (robert.letscher@unh.edu)

Supplementary Material

Appendix: Abbreviation & Definitions

ALOHA: Hawaiian Ocean Time-series station in the subtropical North Pacific

ANCP: Annual net community production

AOU: Apparent oxygen utilization. AOU = $O_{2sat} - O_{2meas}$ the difference between O_2 saturation at a given temperature, salinity, and pressure with the measured O_2 concentration

BATS: Bermuda Atlantic Time-series station in the subtropical North Atlantic

CFC-11 (-12): Chlorofluorocarbon-11 (-12)

γ^n: Neutral density

DCM: Deep chlorophyll maximum

DIC: Dissolved inorganic carbon

DOC: Dissolved organic carbon

DOM: Dissolved organic matter

DON: Dissolved organic nitrogen

DOP: Dissolved organic phosphorus

Ez: Euphotic zone

f_{DOM}: Fraction of oxygen consumption attributable to DOM remineralization

$$f_{DOM} = \frac{\Delta DOM}{\Delta DOM + \Delta POM} = \frac{rPOM}{rDOM}$$

f_{POM}: Fraction of oxygen consumption attributable to DOM remineralization

GLODAP: Global Ocean Data Analysis Project

H: Thickness in meters of subsurface neutral density layers of interest

NCO: NO tracer corrected for the stoichiometry of carbohydrate synthesis (from Fraga, 2001)

Negative preformed nitrate anomaly: Oxygen consumption without stoichiometric nitrate release in the subsurface

Negative preformed phosphate anomaly: Oxygen consumption without stoichiometric phosphate release in the subsurface

Nitracline: Subsurface depths immediately below the euphotic zone where dissolved nitrate rapidly increases in concentration with depth. Top of the nitracline = the depth where $[NO_3^- + NO_2^-] = 0.5\ \mu M$

NO: Conservative water mass tracer computed from the stoichiometric accumulation of nitrate accompanying oxygen consumption in the ocean interior (from Broecker, 1974). $NO = 9NO_3 + O_2$

Non-Redfield: Elemental stoichiometry of C:N:P:$-O_2$ that differs from that defined by Redfield, 1963 – 106C:16N:1P:–138-150O_2

POM: Particulate organic matter

PON: Particulate organic nitrogen

Positive preformed nitrate anomaly: Oxygen production without stoichiometric nitrate drawdown in the euphotic zone

Positive preformed phosphate anomaly: Oxygen production without stoichiometric phosphate drawdown in the euphotic zone

$preNO_3$: Preformed nitrate. $preNO_3 = NO_{3meas} - AOU/R_{-O2:N}$, where $R_{-O2:N}$ is the stoichiometric ratio of oxygen consumed to N regenerated for the remineralization of Redfieldian organic matter, e.g. 150:16. This formulation is referred to as the "traditional" $preNO_3$ tracer and does not account for the non-Redfield remineralization stoichiometry of DOM

r_{DOM}: The stoichiometric ratio of O_2 consumed per mole of DON remineralized

Residual preformed nitrate: $residual\ preNO_3 = NO_{3meas} - \left(f_{DOM} \cdot \frac{AOU}{rDOM}\right) - \left(f_{POM} \cdot \frac{AOU}{rPOM}\right)$. This formulation updates the computation of the traditional $preNO_3$ tracer to explicitly account for the differing $-O_2$:N stoichiometry of POM versus DOM remineralization. This computation is analogous to that originally proposed by Abell et al. 2000; 2005; however, those authors diagnosed $-O_2$:DON remineralization stoichiometry from analysis of $-O_2$:DOC stoichiometry multiplied by the DOC:DON stoichiometry of the bulk DOM pool. The residual $preNO_3$ tracer as defined in this work explicitly diagnoses the $-O_2$:DON remineralization stoichiometry using O_2 and DON data regression analysis.

Residual preformed phosphate: $residual\ prePO_4 = PO_{4meas} - \left(f_{DOM} \cdot \frac{AOU}{rDOM}\right) - \left(f_{POM} \cdot \frac{AOU}{rPOM}\right)$

rNPN: Residual negative preformed nitrate anomaly. This is a negative value of the computed

residual $preNO_3$ tracer and indicates oxygen consumption in excess of that expected from the revised DOM and POM stoichiometric nitrate release.

rPPN: Residual positive preformed nitrate anomaly. This is a positive value of the computed residual $preNO_3$ tracer and indicates oxygen production in excess of that expected from the revised DOM and POM stoichiometric nitrate drawdown.

$R_{-O2:N}$: Oxygen consumed to N regenerated for the remineralization of Redfieldian organic matter, e.g. 150:16

$R_{-O2:P}$: Oxygen consumed to P regenerated for the remineralization of organic matter in the subtropical North Atlantic

r_{POM}: The stoichiometric ratio of O_2 consumed per mole of PON remineralized

rPPN: Residual positive preformed nitrate anomaly

SOM: Subsurface oxygen maximum found between the base of the mixed layer and the nitracline (from Schulenberger and Reid, 1981; Reid, 1962; Jenkins and Goldman, 1985)

TEP: Transparent exopolymer particles

WOA: World Ocean Atlas

Reference

Reid, J. L.: Distribution of dissolved oxygen in the summer thermocline, J. Mar. Res., 20, 138-148, 1962.

Figure S1.

Annual linear regressions of residual $preNO_3$ [μM] vs. time within the γ^n = 24.2 – 24.7 density layer at station ALOHA from 1989 to 2016. Dashed lines show the time interval exhibiting residual negative $preNO_3$ (rNPN) trends each year.

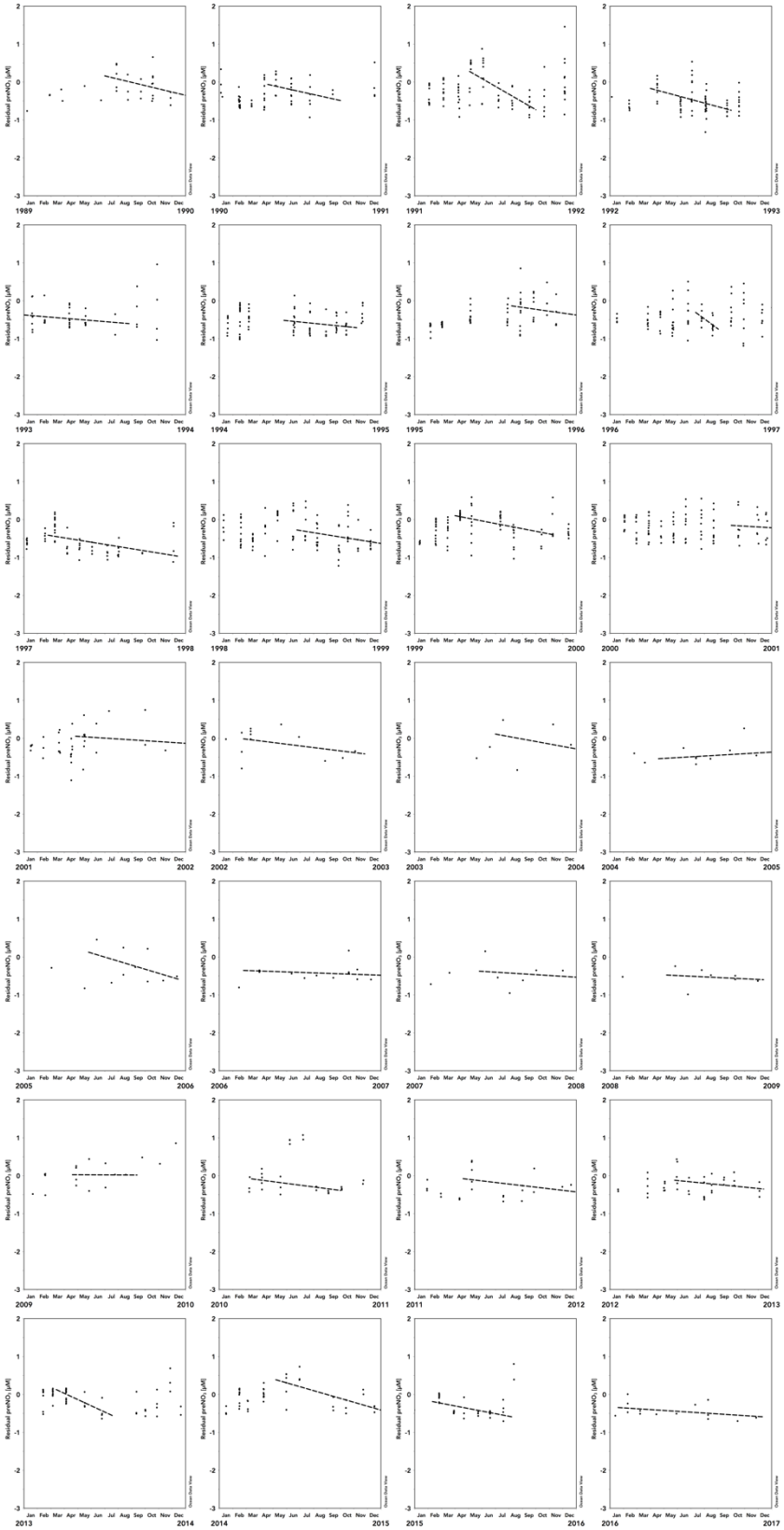

Figure S2.

Annual linear regressions of residual $preNO_3$ [μM] vs. time within the γ^n = 24.7 – 25.2 density layer at station ALOHA from 1989 to 2016. Dashed lines show the time interval exhibiting residual negative $preNO_3$ (rNPN) trends each year.

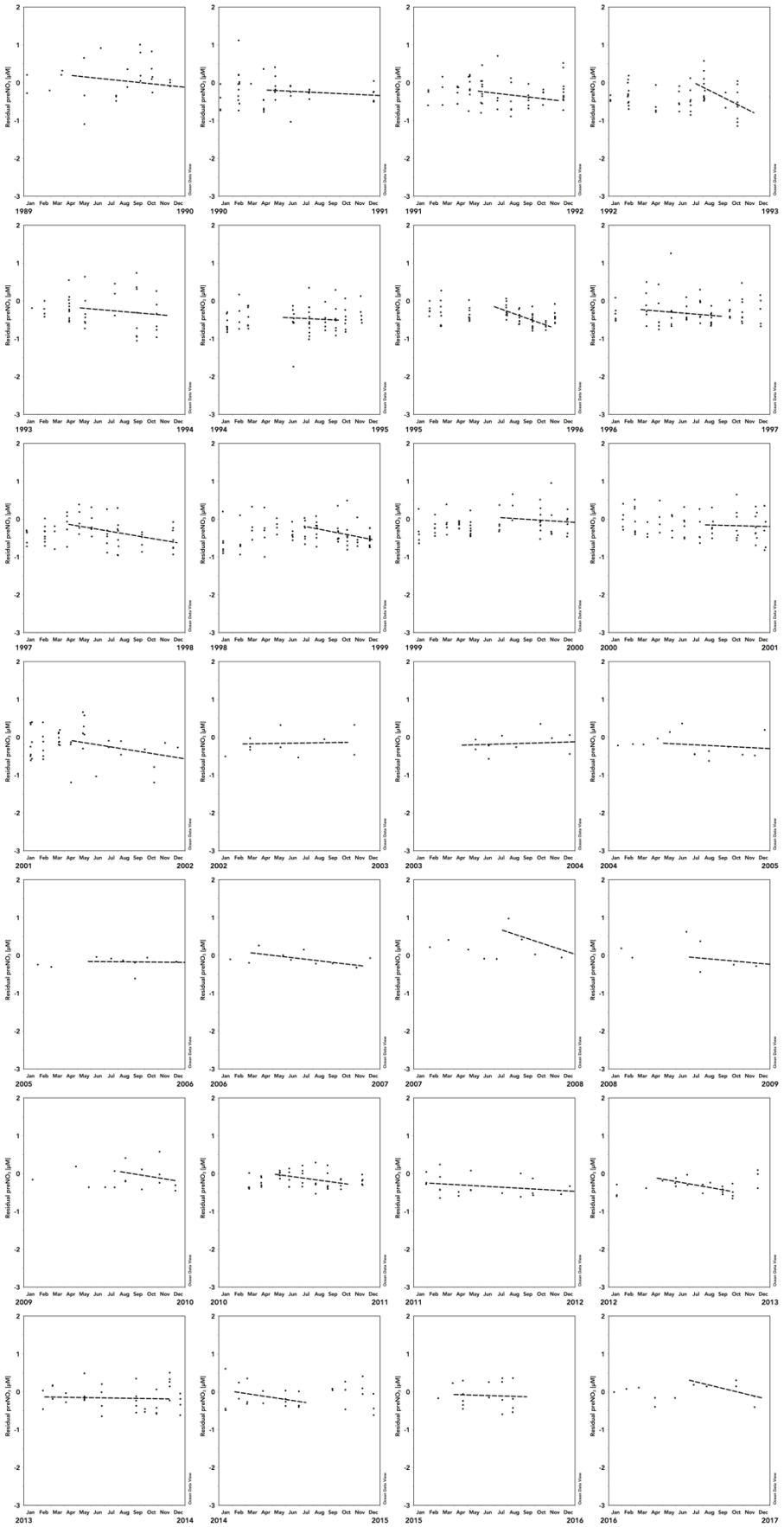

Figure S3.

Annual linear regressions of residual $preNO_3$ [μM] vs. time within the 0 – 100 m depth layer at station ALOHA from 1989 to 2016. Dashed lines show the time interval exhibiting residual positive $preNO_3$ (rPPN) trends each year.

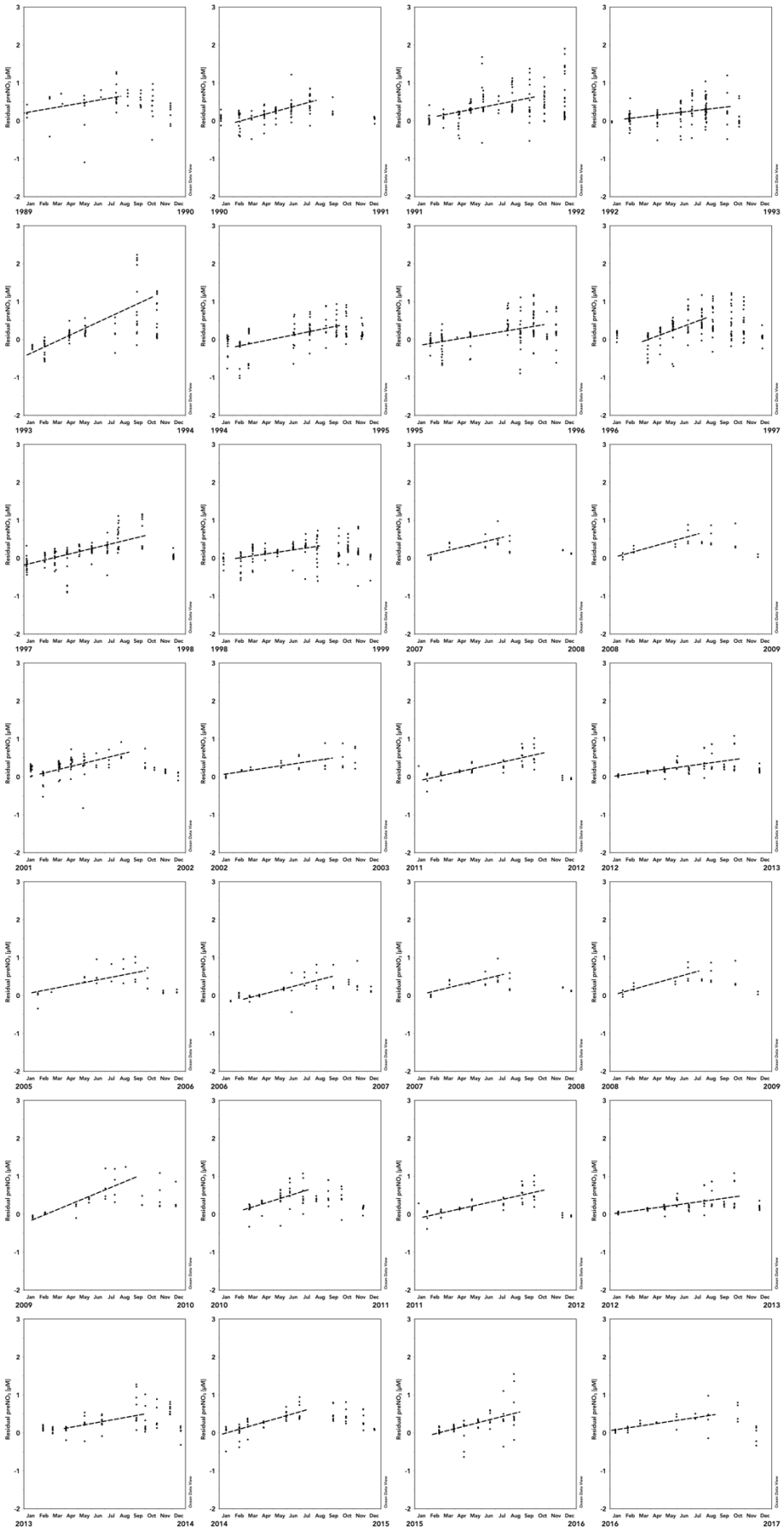

Figure S4.

Annual linear regressions of residual $preNO_3$ [μM] vs. time within the γ^n = 25.8 – 26.3 density layer at the BATS station from 1993 to 2016. Dashed lines show the time interval exhibiting residual negative $preNO_3$ (rNPN) trends each year.

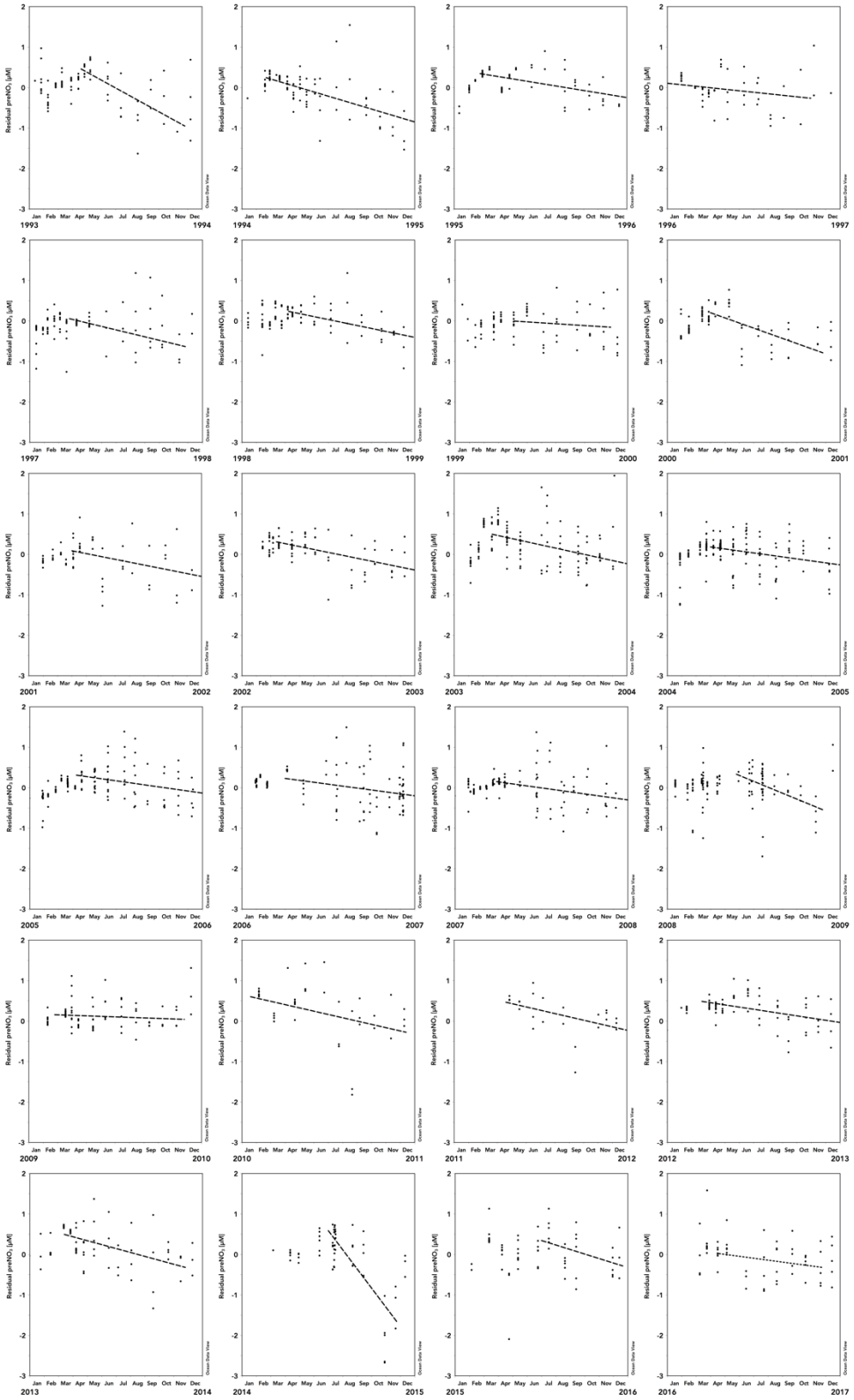

Figure S5.

Annual linear regressions of residual $preNO_3$ [μM] vs. time within the 0 – 80 m depth layer at the BATS station from 1993 to 2016. Dashed lines show the time interval exhibiting residual positive $preNO_3$ (rPPN) trends each year.

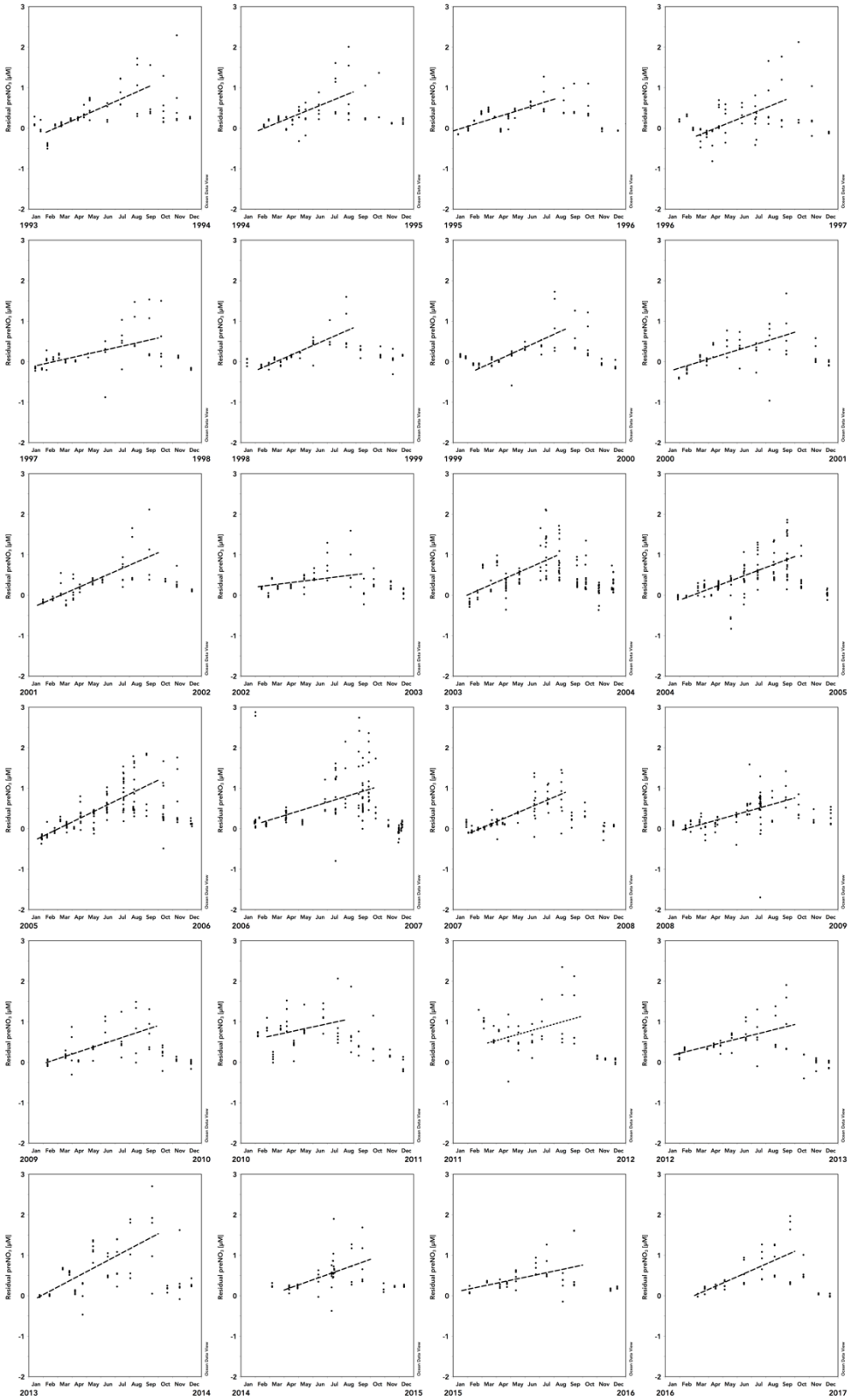

Figure S6. Residual $preNO_3$ [µM] on the neutral density $\gamma^n = 26.5$ surface in the North Atlantic. Residual $preNO_3$ is calculated using the values of f_{DOM} and r_{DOM} determined from the BATS station in Table 1 with a value of $r_{POM} = 10.6$. The dissolved O_2 and nitrate + nitrite for this calculation are from the World Ocean Atlas 2013 annual climatology. The bottom plots show residual $preNO_3$ [µM] versus CFC-11 and CFC-age [years] with depth [m] in color. The BATS station and its data point are highlighted on each plot. The bottom plots including CFC data are from the GLODAP v2 dataset plotted in the domain of the North Atlantic map (top plot).

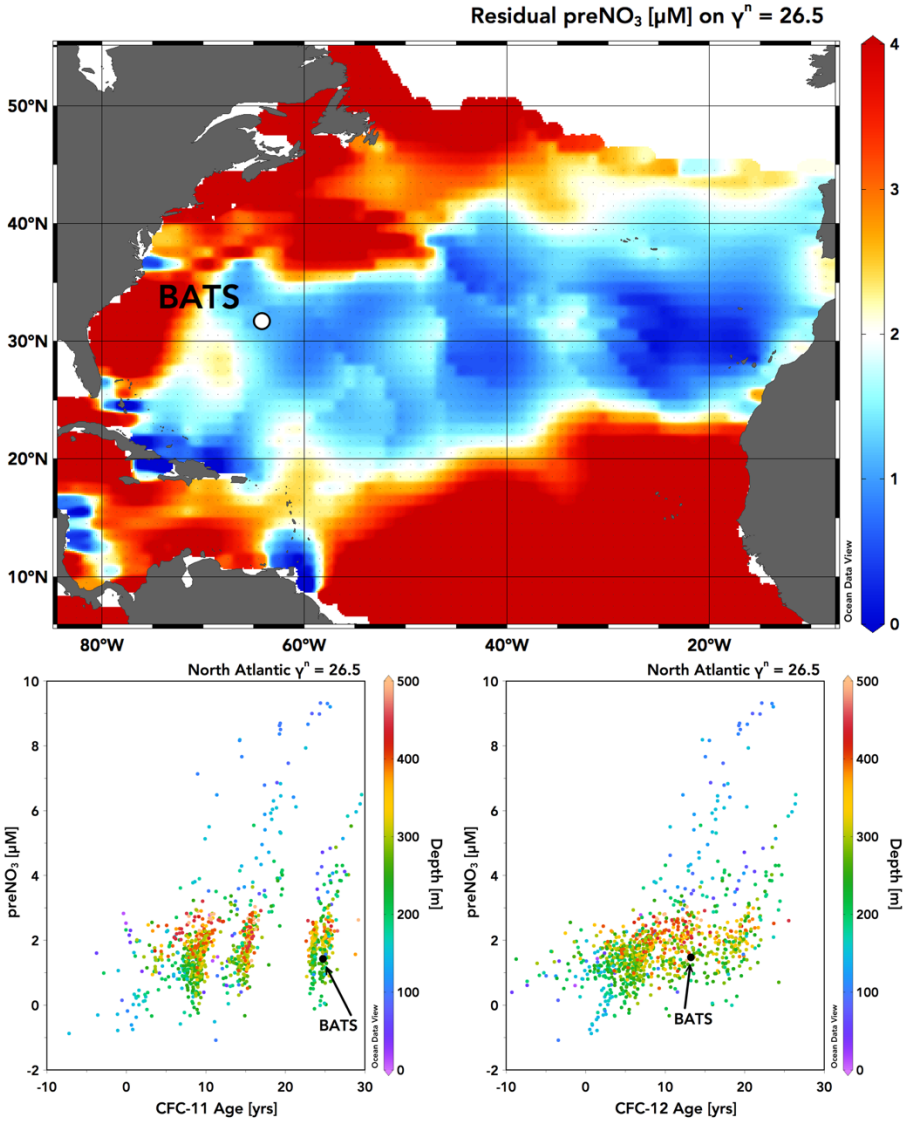

Figure S7. Residual preNO$_3$ [µM] on the neutral density $\gamma^n = 26.0$ surface in the North Atlantic. All datasets and calculations are performed analogous to those detailed for Figure S1.

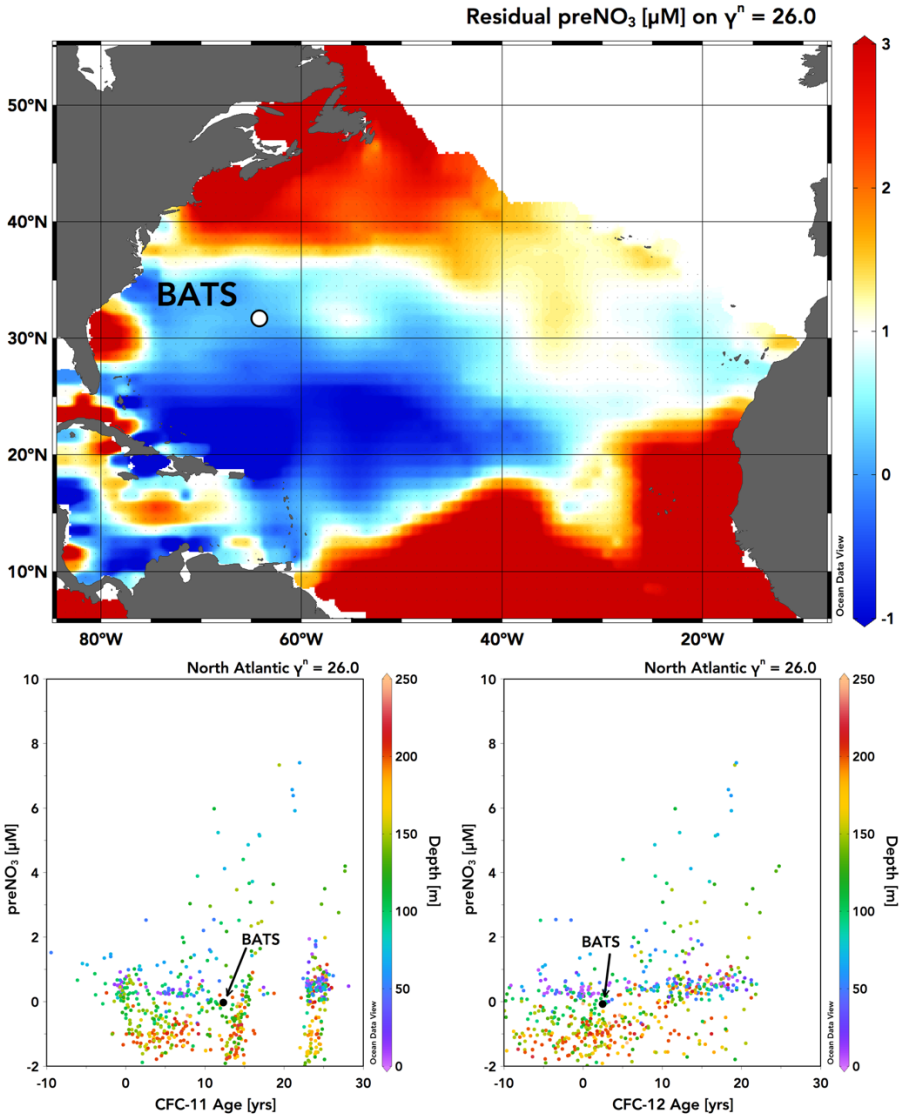

Figure S8. Residual $preNO_3$ [µM] on the neutral density $\gamma^n = 25.4$ surface in the North Pacific. Residual $preNO_3$ is calculated using the values of f_{DOM} and r_{DOM} determined from station ALOHA in Table 1 with a value of $r_{POM} = 10.6$. The dissolved O_2 and nitrate + nitrite for this calculation are from the World Ocean Atlas 2013 annual climatology. The bottom plots show residual $preNO_3$ [µM] versus CFC-11 and CFC-age [years] with depth [m] in color. Station ALOHA and its data point are highlighted on each plot. The bottom plots including CFC data are from the GLODAP v2 dataset plotted in the domain of the North Pacific map (top plot).

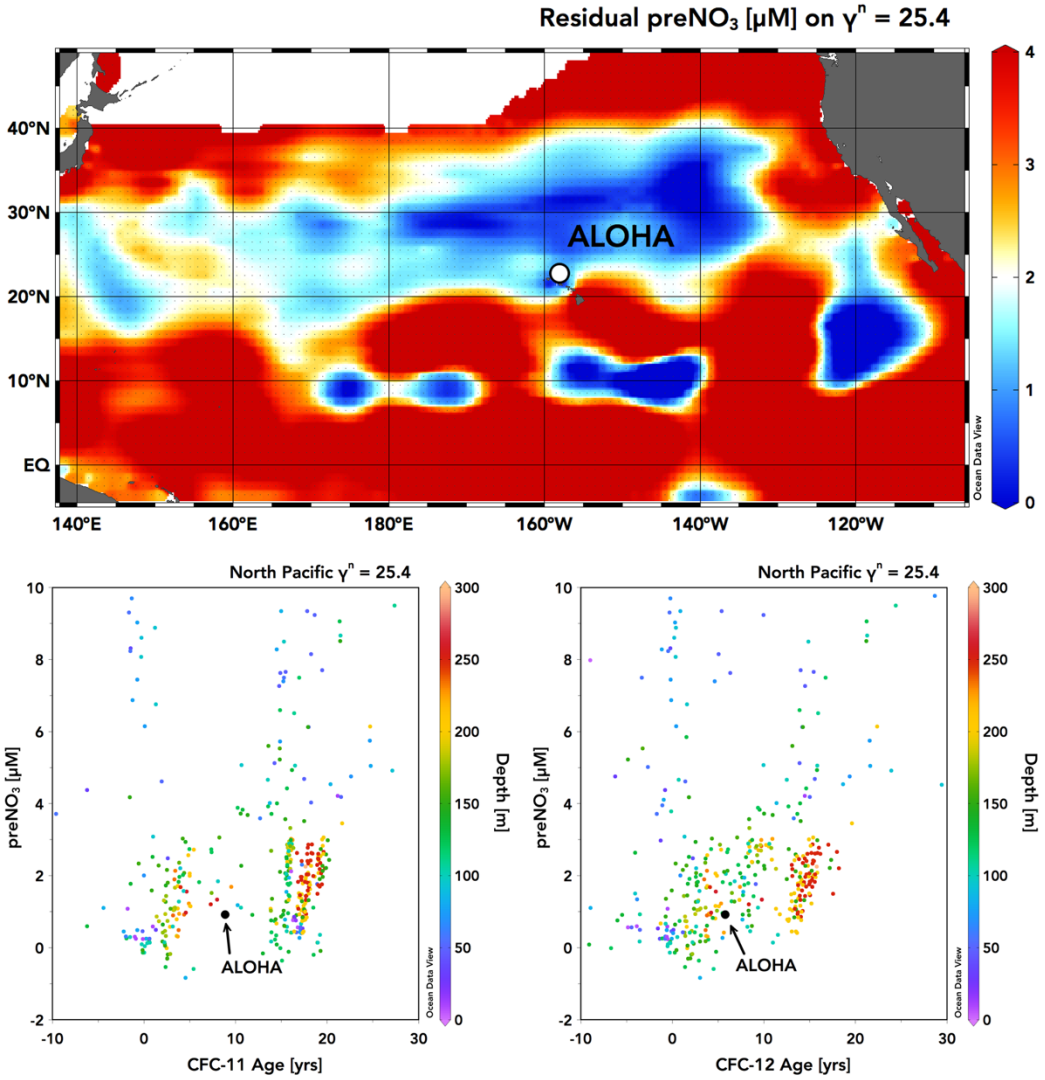

Figure S9. Residual preNO$_3$ [µM] on the neutral density $\gamma^n = 24.7$ surface in the North Pacific. All datasets and calculations are performed analogous to those detailed for Figure S3.

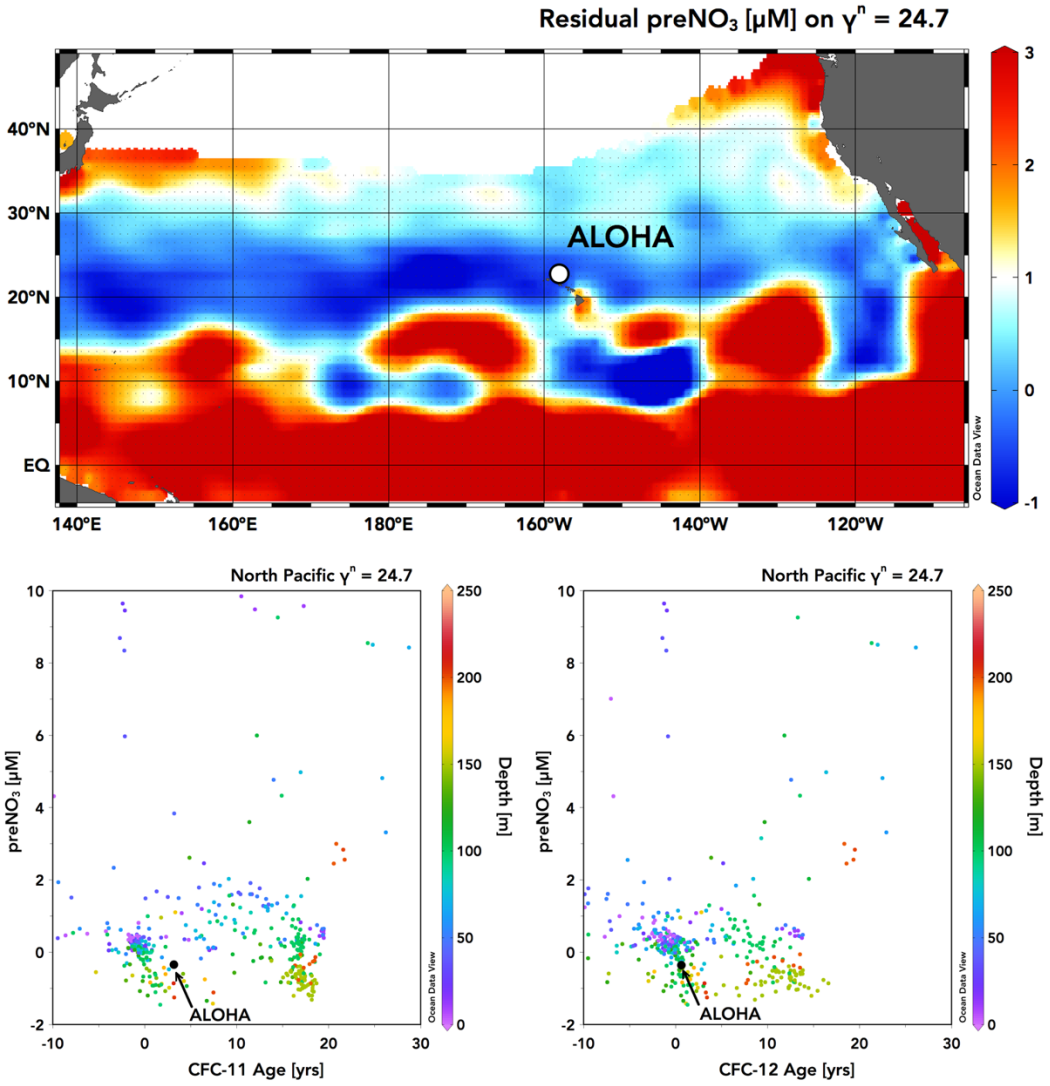

Figure S10. Climatology of a theoretical $prePO_4$ tracer [µM] in the upper 200 m at the BATS station (31.67 ºN 64.17 ºW). Black contour lines show neutral density γ^n = 25.8 and 26.3. The theoretical $prePO_4$ is calculated by finding the value of $R_{-O2:P}$, the stoichiometric ratio of O_2 consumed to PO_4 released for organic matter remineralization, that eliminates the negative $prePO_4$ anomaly present in the subsurface of the time series presented in Figure S6. The value of $R_{-O2:P}$ that eliminates the negative $prePO_4$ anomaly is ~1000:1 (plotted).

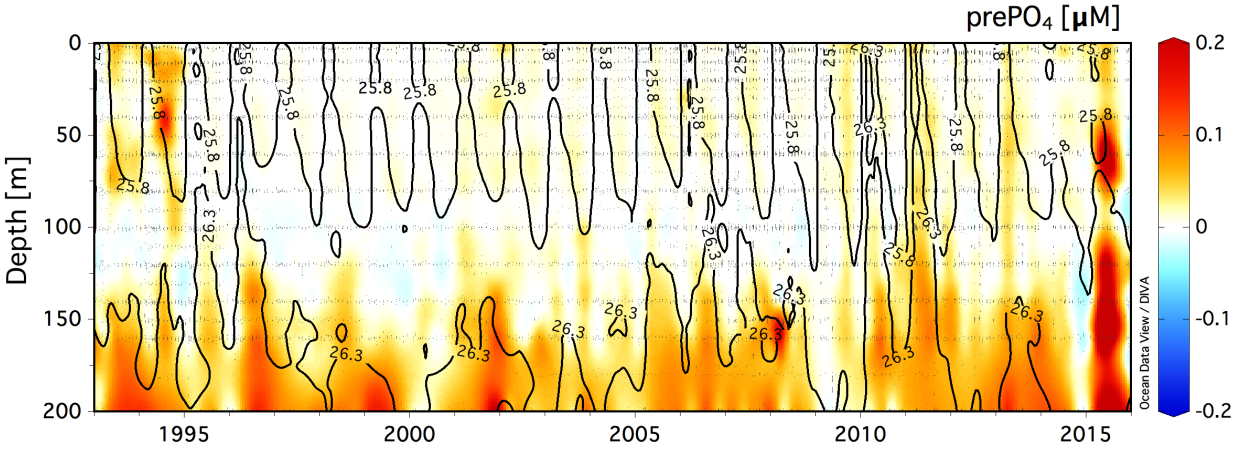

Figure S11. Distribution map for *Pyrocystis* species. Reconfigured from Semina et al. (1977) to remove other species presented on the same figure. Black crosses from Semina et al. (1977) have in some cases been darkened for clarity. White H is Station ALOHA of the Hawai'i Ocean Time-Series. The white B is the Bermuda Atlantic Time-Series. The data are largely from Soviet era oceanographic cruises emphasizing the western Pacific and Indian Ocean. More recent observations in the Sargasso Sea at Bermuda are noted in the text.

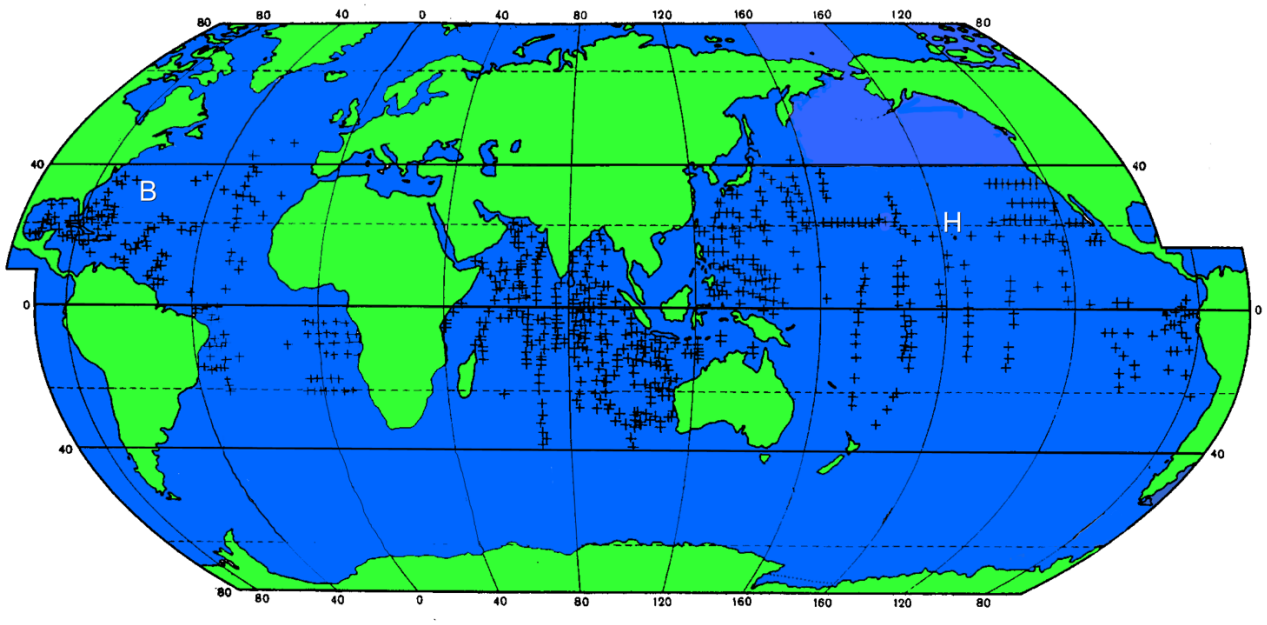

Figure S12. Distribution map for *Ethmodiscus* species. Reconfigured from Mikkelsen (1977) with additional data. Colored boxes with letters are data from Mikkelsen (1977); references can be found there. Red boxes are literature observations added here. Due to the high density of data and scale of the map, the red boxes indicate the range covered by the records. The maps of Belyayeva (1968, 1970), Ricard (1970), and Mikkelsen (1977) provide more detailed presentations. Data from Cleve (1900), Ricard (1970), Belyayeva (1968, 1970), Swift (1973), Swift et al (1973), Swift et al. (1981), Rivkin et al (1984), Villareal (1993), Villareal and Carpenter (1994), Villareal et al (1999a), Villareal (2004), Villareal et al. (2014), Villareal et al (2007).

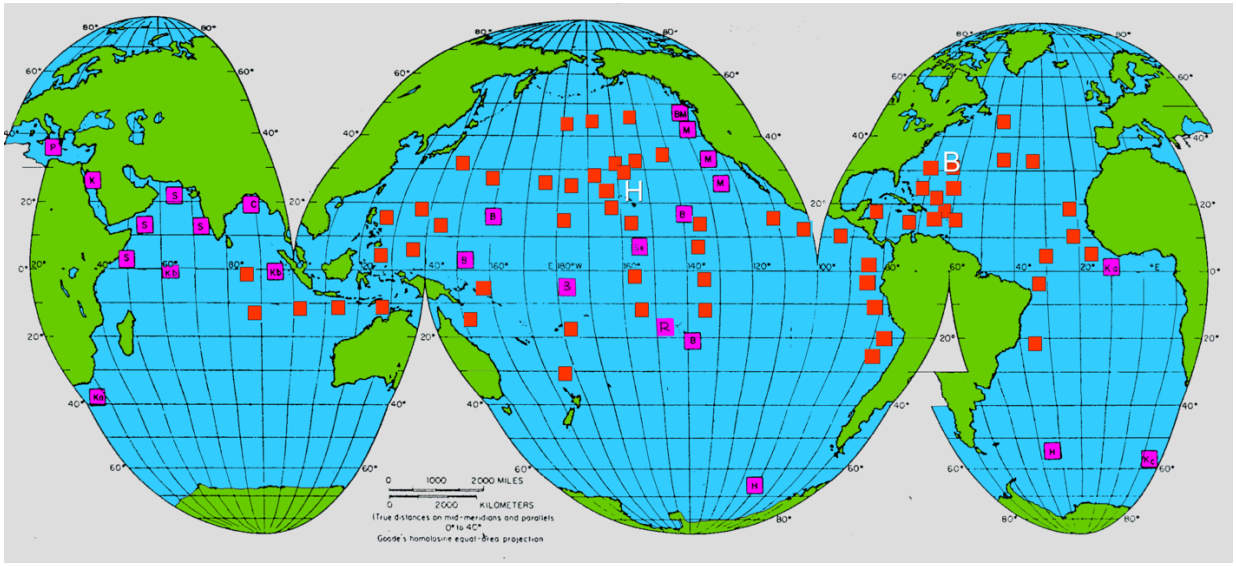

Figure S13. *Rhizosolenia* mat distribution. Nineteenth century reports are from deckboard observations; modern reports are largely based on *in-situ* SCUBA observations. Mats are disrupted by nets and bottle collections due to the mat's fragility (Alldredge and Silver, 1982) and reports are more limited than those taxa based on net samples. Data records from Darwin (1860), Wallich (1858), Carpenter et al. (1977), Martinez (1982), Bauerfiend (1987), Villareal and Carpenter (1989), Villareal et al. (1993), Cowen and Holliday (1996), Villareal et al. (1996), Shipe et al (1999), Villareal et al (1999b), Singler and Villareal (2005), Pilskaln et al (2005), and Villareal et al (2014). Anecdotal data (Cowen and Bruland cited by Alldredge and Silver, 1982) noted mats in both the N. and S. Pacific along a transect from Hawai'i to Tahiti (diver observations; Bruland, pers. comm.). Question marks indicate uncertainty in the location, not the identity. Venrick (1969) noted *Rhizosolenia* mats from deckboard observations in the eastern N. Pacific gyre as well as reports off coastal California (R.W. Eppley, cited in Carpenter et al., 1977).